COCOSYS analysis on aerosol wash-down of THAI-AW3 experiment and generic containment

Fangnian Wang [a,*], Xu Cheng [a], Sanjeev Gupta [b]

[a] Institute for Applied Thermofluidics (IATF), Karlsruhe Institute of Technology (KIT), Germany
[b] Becker Technologies GmbH, Germany

ARTICLE INFO

Keywords:
COCOSYS
Aerosol wash-down
THAI-AW3 experiment
Generic containment

ABSTRACT

During severe accidents, fission products as aerosols are released into the containment and consequently deposited on walls. The condensate flow on walls could wash the deposited aerosols downwards to the sump. Therefore, the aerosol wash-down process on walls is significant to evaluate radioactive source term distribution in nuclear containment. In this paper, the containment code COCOSYS coupled with aerosol wash-down model AULA and condensate coverage model CONRAG is used to analyze the aerosol wash-down process of THAI-AW3 experiment and 'Generic Containment'. THAI-AW3 experiment was conducted by Becker Technologies to investigate insoluble aerosol wash-down behavior from the vertical, quasi-horizontal surfaces, and a small puddle. The COCOSYS calculated results shows the aerosol wash-down is predicted well, as well as the thermal-hydraulics in THAI-AW3 experiment. There are no significant differences of aerosol wash-down efficiency between the calculation and measurement. The acceptable COCOSYS is to enable further analysis on the aerosol wash-down process of the Generic Containment within SARNET2 activity under a full severe accident scenario in order to test the aerosol wash-down model. The evolutions of the containment' thermal-hydraulics are analysed. The calculation offers the aerosol distribution, the aerosol wash-down mass, and the aerosol distribution inside containment over time. The comparisons with previous COCOSYS simulations indicate that the modification of COCOSYS, e.g. the coupling with condensate coverage model CONRAG, is necessary to investigate the aerosol wash-down.

1. Introduction

During severe accidents, fission products are generated due to core degradation inside Reactor Pressure Vessel (RPV) or molten core-concrete interactions (MCCI) outside RPV, and released into the containment with a large amount of steam and non-condensable gases. Together with the condensing steam, aerosols are transferred on cold walls (Weber et al., 2015). The condensate flow washes down the aerosols, and transports them into lower compartments or sumps. The aerosol wash-down process influences the distribution of the fission products. The source term distribution is important to assess radiation damages of local components like electronic devices, seals, etc. Moreover, the amount of fission products transported to the sump is of high interest, because the decay heat released into sump has a major influence on the containment thermal-hydraulics and the amount of trapped aerosols in the sump determines the available fission products inventory in the containment atmosphere. Therefore, there is also a large impact on the possible source term to the environment.

COCOSYS code is a part of the GRS code system AC^2, designed for simulating relevant phenomena, processes, and conditions expected during design basis and severe accidents inside the containment (Klein-Heßling et al., 2015). The containment of a nuclear reactor building is the last barrier to prevent a release of radioactive materials to the environment. One key aspect of COCOSYS is the extensive consideration of interactions between various phenomena, such as thermal-hydraulics, hydrogen combustion, aerosol and fission product behavior, and molten core-concrete interaction. The models implemented in COCOSYS are based on a lumped parameter (LP) concept. The compartments or rooms of a power plant, a test facility, or any other building are subdivided into control volumes to be analysed, which are connected by so-called junctions. The temperatures and masses of the specified components (e.g. gases, steam, and water) define the thermodynamic state of a control volume. The mass and energy balances are solved while the momentum balance of the gas flow inside

* Corresponding author.
E-mail address: fangnian.wang@kit.edu (F. Wang).

Nomenclature

A	wall area, m^2
$C_{i,c}$	correction factor of inclination and cohesion
c_{ae}	deposited aerosols load on surface, kg/m^2
$c_{ae,0}$	initial deposited aerosols load on surface, kg/m^2
d_p	particle diameter, m
F_C	cohesive force, N
F_W	buoyant weight of particle, N
g	gravity acceleration,$9.8 m/s^2$
Ka	Kapitza number
k_e	erosion rate, 1/s
$k_{e,0}$	erosion constant, 1/s
m_{ae}	remaining deposited aerosol mass on wall, kg
R^*	dimensionless auxiliary parameter
Re	Reynolds number
Re^*	particle Reynolds number
s	density ratio of particle to water
t	time, s
u	rivulet (condensate) velocity, m/s
$\overline{u}$	average rivulet (condensate) velocity, m/s
u^*	rivulet (condensate) shear velocity, m/s
u_c^*	critical shear velocity of particle, m/s
$\dot{V}$	volume flow rate per width, $m^3/(m{\cdot}s)$

Greek symbols

α	inclination angle, °
δ	rivulet (condensate) thickness, m
$\overline{\delta}$	average rivulet (condensate) thickness, m
ε	rivulet (condensate) coverage
θ_e	equilibrium contact angle, °
μ	water viscosity, Pa·s
μ_c	Coulomb friction coefficient
ν	kinematic viscosity, m^2/s
ρ	water density, kg/m^3
σ_{LG}	surface tension between water and air, N/m
τ_c^*	dimensionless critical shear stress
$\tau_{c,o}^*$	dimensionless critical shear stress of horizontal bed

control volumes is not considered. For walls (structures), a one-dimensional heat conduction equation is solved (Klein-Heßling et al., 2015).

The aerosol wash-down process interacts with thermal-hydraulics and aerosol particle transport process in the containment (Weber et al., 2015). In the containment code COCOSYS, the thermal-hydraulics and the aerosol wash-down process are currently modelled (Klein-Heßling et al., 2015). For instance, the aerosol wash-down model for insoluble aerosols **AULA** (German: "**A**bwaschen **u**n**l**öslicher **A**erosole") simulates the erosion of insoluble aerosols by flowing condensate. The erosion takes place if the flow shear velocity at the wall exceeds the critical threshold (Shields' criterion in sediment transport theory (Guo, 2002)). Comparing with the previous aerosol wash-down model AULA, the current model is extended to be valid for the inclined walls and the cohesive aerosols, which is validated by the laboratory scale experiment THAI-AW3-LAB (Wang and Cheng, 2020).

Meanwhile, the condensate coverage (water-covered area fraction) is an important parameter that indicates how much area is wetted, where the aerosol wash-down takes place. The **CON**densate cove**RAG**e model **CONRAG** is proposed in our previous work (Wang and Cheng, 2019, 2020), which depends on the condensate volume flow rate per width, contact angles, surface inclination, and fluid properties.

However, in order to assess the performance of the extended aerosol wash-down model AULA coupled with the new condensate coverage model CONRAG in COCOSYS code (the aerosol behavior module New_AFP 2019.10.07 GRS delivered to KIT), a further validation against an integral aerosol wash-down experiment is carried out. In addition, the modified COCOSYS is applied in a 'Generic Containment' within the SARNET activity under severe accident conditions (Kelm et al., 2014), in order to evaluate the capability of the new models.

2. Aerosol wash-down model

The wash-down of insoluble aerosols, like Ag and AgO_x aerosols, are complex because the wash-down process depends on the particle properties (size and density), particle porosity, surface inclination (wall and floor), thermal-hydraulic conditions (flow patterns, condensate coverage, and fluid properties), etc.

The aerosol wash-down model AULA (Weber, 2011; Weber et al., 2015) is based on an approach used in geology to describe the transport of sediments in water flow. A criterion (so called Shields criterion, (Shields,1936)) is adopted, which states that particles erode if the flow shear velocity exceeds the critical shear velocity determined by particles. The AULA model suggests the surface load (surface density) (called 'concentration' in Weber et al., 2015) of deposited aerosols on walls, c_{ae}, kg/m^2, decreases as an exponential function:

$$\frac{dc_{ae}}{dt} = -k_e \cdot c_{ae} \tag{1}$$

where k_e, 1/s, is the erosion rate, i.e. the characteristic time of the erosion process, has to be measured for each specific condition. This aerosol mass erosion rate is introduced by (Ariathurai, 1977) for cohesive particles:

$$k_e = \begin{cases} k_{e,0}\left(\frac{u^{*2}\ u_c^{*2}}{u_c^{*2}}\right), u^* > u_c^* \\ 0, u^* \le u_c^* \end{cases} \tag{2}$$

where $k_{e,0}$ is an erosion constant that has to be estimated. This constant depends on the aerosol particle and flow properties (Weber et al., 2015; Amend and Klein, 2017, 2018). According to the Shields criterion, the erosion of particles takes place if the flow shear velocity u^* is beyond the critical shear velocity u_c^* of particles; otherwise, there is no erosion.

The integral form of the surface load of deposited aerosols c_{ae} can be obtained by Eq. (1). The remaining deposited aerosol mass on water-covered area is:

$$m_{ae} = A \cdot \varepsilon \cdot c_{ae,0} \cdot e^{(\ k_e t)} \tag{3}$$

where A is the whole wall area, and ε is the condensate coverage. $c_{ae,0}$ is the initial surface load of deposited aerosols, kg/m^2.

In AULA, the deduction of the shear velocity u^* depends on the type of flow. Because of the slight roughness of the decontamination paint surface (a typical structure surface in containment), smooth turbulent flows can be expected (Weber et al., 2015). The shear velocity for hydraulically smooth flows is calculated by using a parabolic flow velocity profile (Hillebrand, 2008).

$$u^* = u\frac{0.41}{ln\left(\frac{u^*\delta}{\nu}\right)+5.25} \tag{4}$$

where u and δ are the condensate (e.g. rivulet, film) velocity and thickness respectively. The 0.41 is Karman constant. The u^* can be solved by the iteration of the implicit Eq. (4).

As seen in Eq. (2) and Eq. (3), the critical shear velocity and the condensate coverage have great importance of the aerosol wash-down efficiency. These two parameters are described as follows:

- Critical shear velocity

The critical shear velocity of particle is:

$$u_c^* = \sqrt{\tau_c^*(s-1)gd_p} \tag{5}$$

where d_p is the particle diameter. g is the gravity acceleration. s is the density ratio of particle to water:

$$s = \rho_p/\rho \tag{6}$$

where ρ is the water density. The co-called critical Shields parameter, namely the dimensionless critical shear stress, is:

$$\tau_c^* = C_{i,c} \cdot \tau_{c,o}^* \tag{7}$$

where $C_{i,c}$ is the combined correction factor for surface inclination and particle cohesion.

In AULA, one empirical correlation of the horizontal and non-cohesive particle bed (Guo, 2002) is applied. This empirical correlation is fully validated for a large range of particle size and flow velocity. The empirical critical Shields parameter of horizontal particle bed, is:

$$\tau_{c,o}^* = 0.1(R^*)^{\frac{2}{3}} + 0.054\left[1 - e^{\left(-0.1(R^*)^{\frac{2}{3}}\right)}\right] \tag{8}$$

where the dimensionless auxiliary parameter R^* is:

$$R^* = \frac{d_p\sqrt{0.1(s-1)gd_p}}{\nu} \tag{9}$$

where ν is the water kinematic viscosity.

For the normal particle bed, the dimensionless critical shear stress is corrected by the consideration of surface inclination and particle cohesion:

$$C_{i,c} = \left(cos\alpha - \frac{sin\alpha}{\mu_c} + \frac{F_c}{F_w}\right) \tag{10}$$

The new combined correction factor $C_{i,c}$ of surface inclination and particle cohesion is derived by the aerosol force analysis (Wang and Cheng, 2020). α is the surface inclination angle. μ_c is the Coulomb friction coefficient. $\frac{F_c}{F_w}$ is the force ratio of cohesive force to particle buoyant weight.

- Condensate coverage model

The estimation of condensate coverage is a necessary boundary condition for calculating aerosol wash-down. A new condensate coverage model CONRAG is proposed. The modelling approach is presented in (Wang and Cheng, 2019) and the new empirical correlation is proposed and validated in (Wang and Cheng, 2020), which is expressed as:

$$\varepsilon = 0.26 \cdot Re^1 Ka^{0.6}(1 - cos\theta_e)^{0.6}(sin\alpha)^{0.2} \tag{11}$$

where the Reynolds number $Re = \frac{4\rho\dot{V}}{\mu}$, and the Kapitza number $Ka = \sigma_{LG}\left(\frac{\rho}{g\mu^4}\right)^{1/3}$. θ_e is the equilibrium contact angle and α is the surface inclination angle, which are physically influence the surface tension force and gravitation in the forms of $(1 - cos\theta_e)$ and $sin\alpha$ respectively. The condensate coverage is proportional to $(sin\alpha)^{0.2}$. The average film thickness $\overline{\delta} \propto (sin\alpha)^{-0.4}$ and velocity $\overline{u} \propto (sin\alpha)^{0.2}$ so that the condensate coverage can be scaled as $\varepsilon \propto \frac{\dot{V}}{\overline{u}\cdot\overline{\delta}} = (sin\alpha)^{0.2}$. $\dot{V}$ is the volume flow rate per length. It should be clarified that the coverage model is not valid for horizontal surface since the condensate flow is drove by the gravitation. If the surface is horizontal (means the inclination angle is zero), there is no gravitational force to drive the condensate falling along the surface. The CONRAG is validated by the inclined walls of 2°, 10°, 20°, 60° and 90°, and the steel surface both with and without the pre-deposited aerosols. The validation against the experimental data indicates a good agreement with around ±25% deviation (Wang and Cheng, 2020). This coverage correlation is eventually coupled to calculate the aerosol wash-down process. From reactor application point of view, the aerosol-loading behavior, e.g. the surface-loading, particle properties and surface properties, influences the CONRAG model by means of the contact angle. The effect of the contact angle on the condensate coverage was presented in our previous work (Wang and Cheng, 2020).

3. Validation against THAI-AW3 experiment

3.1. THAI-AW3 experiment

THAI is a technical-scale containment test facility designed and built to address fission product and thermal-hydraulic issues under design basis accident and severe accident conditions. A series of aerosol wash-down experiments including THAI-AW, AW2, AW3, and AW4 is carried out in THAI project (Gupta and Langer, 2009; Gupta et al., 2012; Freitag et al., 2016). The aerosol wash-down experiments have been performed to investigate the aerosol wash-down behavior of insoluble/soluble aerosols on surfaces and the water spray effect. The experiment THAI-AW3 has been conducted to investigate the insoluble Ag aerosol wash-down behavior from surfaces, which are the vertical surfaces, quasi-horizontal tray (plate with small inclination 2°), and a small puddle. The objectives of THAI-AW3 are to identify the dominant parameters and transport mechanisms of the insoluble Ag aerosol deposited on walls and to determine the aerosol wash-down efficiency (Freitag et al., 2016).

- THAI facility

The main component of the THAI facility is a cylindrical stainless steel vessel of 9.2 m height, 3.2 m diameter, and total volume of 60 m^3 with exchangeable internals for multicompartment investigations (Gupta et al., 2015). THAI test vessel is installed with internal trays for aerosol wash-down on quasi-horizontal surfaces. The vessel is designed for a maximum overpressure of 14 bar at 180 °C and can withstand moderate hydrogen deflagrations. The cylindrical part of the THAI vessel is equipped with three independent heating/cooling systems over the height for controlled wall temperature conditioning by means of external thermal oil circuits. The sump water can be heated and recirculated at different flow rates. The vessel structures are made of stainless steel and completely enveloped by a 120 mm rock wool for thermal insulation. The inner wall is 22 mm thick. The 16.5 mm gap between the vessel walls is filled with thermal oil of the wall heating/cooling system. The outer wall is made of 6 mm thickness stainless steel. Vessel top and bottom are formed by dished heads (with wall thickness 30 mm), both of which are penetrated in the vessel by a top cylinder with diameter 1.54 m and a bottom cylinder with diameter 1.368 m respectively. The top cylinder is joined by a 120 mm thick top flange. The bottom cylinder is closed by a 16 mm thick dished head. More details of the THAI geometry can be found in (Freitag et al., 2016).

- Test procedure and test conditions

The test procedures of THAI-AW3 are established under well-controlled test conditions (Freitag et al., 2016). Time t = 0 h corresponds to the start time of steam injection. The procedures during the test, as described in Fig. 1, are introduced as below:

Phase 0 is the preconditioning with time duration 13.83 h (start at t = 42.08 h) to have initial conditions for aerosol injection. The heating system (jackets) starts with a target wall temperature of 128 °C except the sump compartment, which is set to 110 °C.

Phase 1 is the aerosol injection and deposition phase with time duration 28.25 h. Three times of aerosol injections with the carrier gas 'air' are activated, so that the vessel pressure increases suddenly three times accordingly. The continuous slow increase until t = -6.383 h is mainly due to the injection of air used for purging the laser extinction measurement systems (Freitag et al., 2016). The total mass of silver injected in the THAI vessel is 465.5 g. The -mass-median-diameter (i.e. the average particle diameter by mass) is about 1.1 μm. Then the vessel atmosphere remains quiescent to allow the deposition of aerosols on the surfaces. The coupons are removed at time t = 6.37 h to quantify the Ag aerosol surface load. The aerosol surface load is between 32.7 g/m^2 and 36.3 g/m^2. The average surface load of these 10 coupons is about 35.1 g/m^2. Considering the total injected amount of 465.5 g silver aerosols, the average load on the vertical walls can be approximated 2.5 g/m^2. The vessel pressure is regulated by opening the pressure relief valve to reduce to about 1 bar. Air injection starts to establish the vessel pressure after closing the vessel.

Phase 2 is the aerosol wash-down with time duration 3.32 h. The time t = 0 h indicates the start of steam injection at an elevation of 2.4 m by a pipe with inner diameter 44 mm. The steam mass flow rate maintains constantly at about 17 g/s.

Actually, there is a phase 3 of THAI-AW3, namely the iodine/silver interaction in a water sump, but it is not the topic discussed in this paper. Here, we concentrate on the aerosol wash-down process, so that the phase 0 and 1 are the initial condition of our COCOSYS simulation. Two parameters of aerosol wash-down model required in the simulation of THAI-AW3 are obtained based on the knowledge of our previous validation with laboratory scale experiment THAI-AW3-LAB (Wang and Cheng, 2020), e.g. the effective particle density is 1550 kg/m^3, the erosion constant $k_{e,0} = 0.03$ in Eq. (2), the combined correction factor $C_{i,c}$ for surface inclination and particle cohesion is unit one. That is because the aerosol of Ag used in both expeirments are the same, and it is reasonable to adopt these constants in the current validation instead of adjusted values. However, in current case the rivulet for aerosol wash-down occurs on pre-wetted surface is assumed (because steam condensation happens before aerosol wash-down) so that the equilibrium contact angle is recommended 14°, which is a measured value on pre-wetted surface coated decontamination paint. It is meaningful to specify the range the constants, e.g. contact angle and erosion constant, for the later model/code users. However, these constants usually are obtained by experiments. The sensitivity analysis of aerosol characteristics was done (Wang and Cheng, 2020), concluding the effects of aerosol properties and the surface inclination for the aerosol wash-down ecciciency.

3.2. COCOSYS model of THAI-AW3

In order to simulate the thermal-hydraulics in THAI facility, it is necessary to subdivide the vessel into a certain number of control volumes. In the current simulation, three levels are used for the upper, middle, and lower cooling jacket compartments individually. The plume shaped control volumes consist of the injection flow path. The side view of the nodalisation is presented in Fig. 2.

The quasi-horizontal tray installed in the vessel consists of 20 individual plates, in which 4 plates create a small puddle (39 mm depth, 26.9 L volume, (Freitag et al., 2018)), as shown in Fig. 3. Each plate is fan-shaped with an angle of 18° and inclined with a downward angle 2°. The surface area of each plate is 0.37 m^2. All quasi-horizontal plates are coated with artificially aged decontamination paint. Four plates have been bypassed by

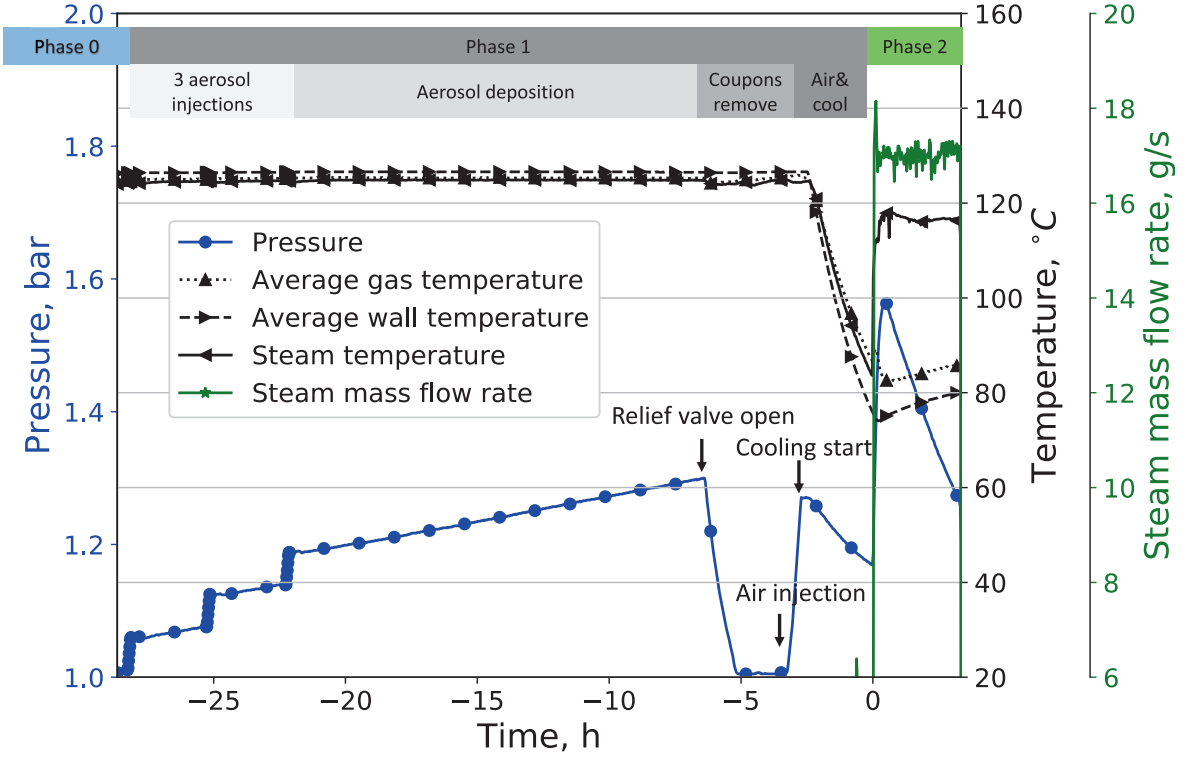

Fig. 1. Test procedures and test conditions of THAI-AW3.

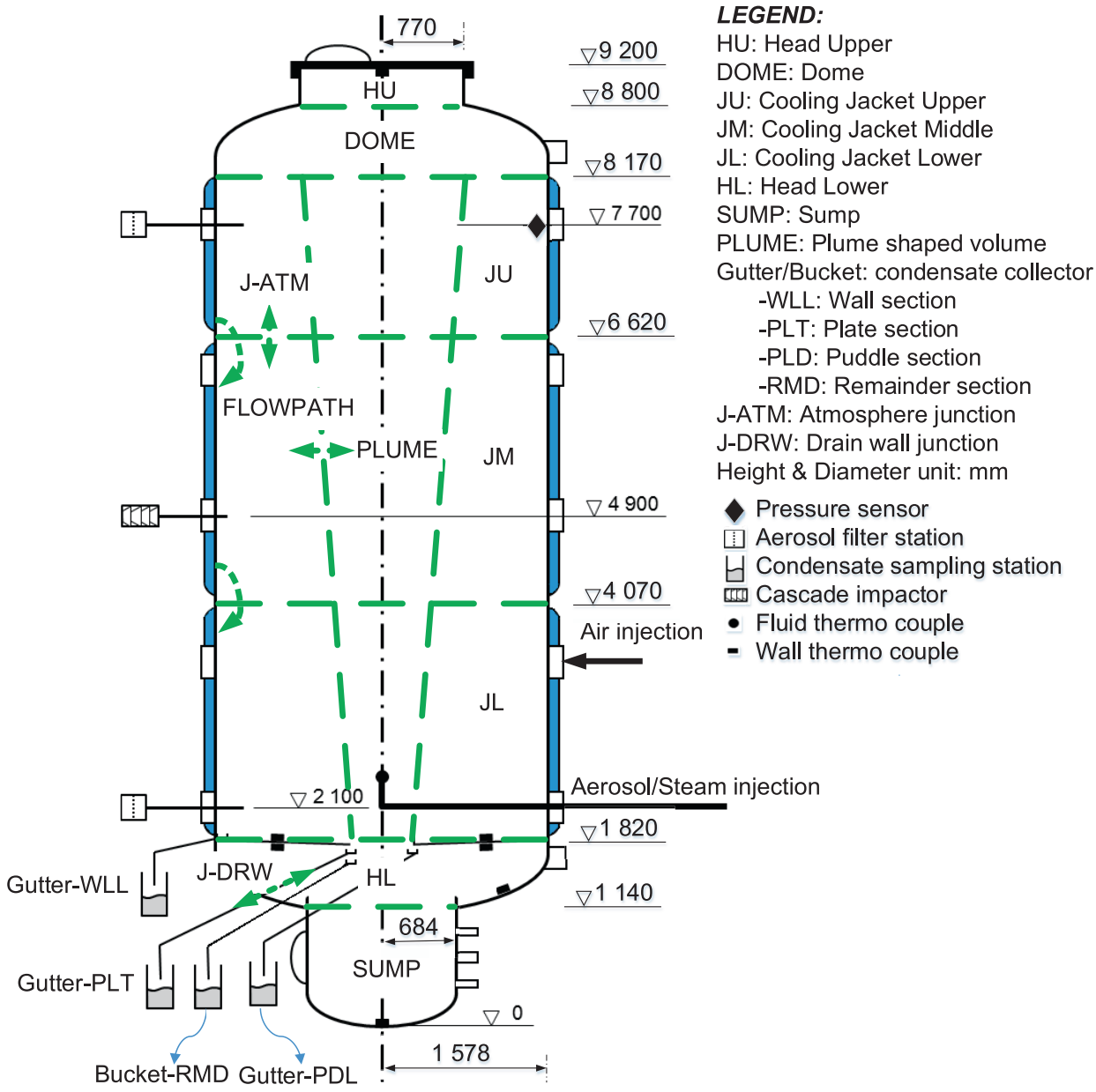

Fig. 2. Nodalisation and side view of THAI-AW3.

installing a condensate gutter, which collects condensate from the vertical wall directly. The remaining plates are flushed by the condensate, which flows directly from the vertical vessel walls to the plates. In order to allow the gas flow path also possible in the horizontal direction, nodalisation is subdivided into 4 sections circumferentially: the vertical wall section of 72°, the combined wall/plate section of 72°, the combined wall/puddle section of 72°, and the combined wall/remainder section of 144°, which in short are wall, plate, puddle, and remainder section respectively. The injection plume zone in the middle. The top view of the nodalisation and experimental information are presented in Fig. 3.

The atmosphere junction type is the standard model to describe atmospheric flow between two connected control volumes (zones). The junction can be a real flow path (like the plume zone to the lower head zone) or a virtual flow path, which results from subdividing of the vessel into several control volumes. For the simulation of the liquid flow from one zone to another, the drain junction model is available. Moreover, the flow path model is adopted to simulate the condensate flow from the upper to the lower structures. Finally, in the current nodalisation model of THAI-AW3, there are 29 zones, 45 atmosphere junctions, 5 drain junctions, and 31 structures.

3.3. Results comparison

The preconditioning and aerosol injection/sedimentation (phase 0 and phase 1) are not included in the calculation, which starts at time t = 0. The aerosol deposition loads provided by experiment are given in the inputdeck, so that the aerosol wash-down model is validated directly without including the simulation uncertainties of the aerosol injection/sedimentation process.

In accordance with the objectives of the aerosol wash-down test, the parameters such as pressure, temperature, aerosol concentration, and condensate flow rate are measured (Freitag et al., 2018). Fig. 4 shows the COCOSYS results of pressure and temperature compared against experimental data. The pressure measure-

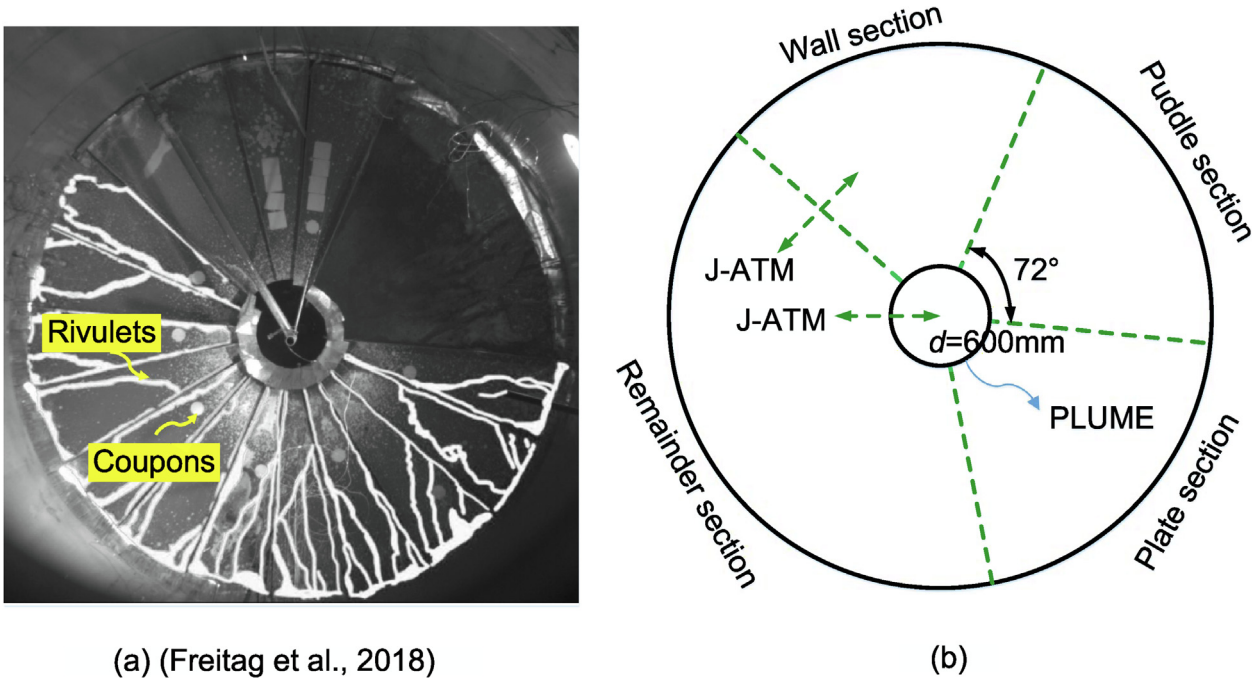

Fig. 3. Top view of THAI-AW3 at elevation 1.82 m: a, experiment; b, nodalisation.

ment is located inside the vessel at level 7.7 m, as shown in Fig. 2. The pressure increases rapidly in the beginning of the test because of the steam injection and the little condensation on walls, but the trend changes in the later phase since the condensation balances the energy released by the steam in the vessel.

A typical set of instrumentation (e.g. thermocouples) for measuring the thermal-hydraulic conditions has been installed inside the THAI vessel. The temperatures of the atmosphere in the vessel are measured over the height and circumference (Freitag et al., 2018). Here, the average gas temperature is taken as the examples for the comparison, as shown in Fig. 4. Both the trend and quantity agree with the experimental data well.

The condensate from each test section (plate, wall, puddle, and remainder, as shown in Fig. 3) are continuously drained into the corresponding gutters attached to each section. Fig. 5 shows the calculated results of condensate mass flow rate agree well with the experimental data, but start a little ahead of experimental data and show slight oscillation, because a part of the condensate (~0.0792 kg) is reserved in each gutter that delays the condensate measurement. In the beginning, the difference of the condensation rate between the wall and plate sections is mainly due to the condensation on the flat plate (due to initial wall temperature less than the steam), but it is also influenced by the inhomogeneity of the power of the cooling system. It is the similar reason for

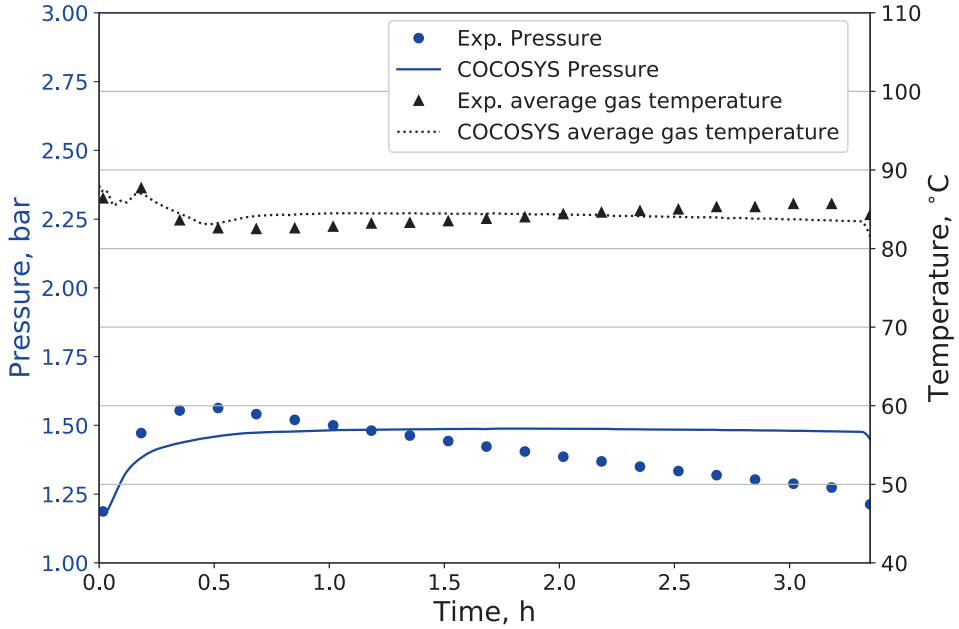

Fig. 4. Pressure and temperature comparison against THAI-AW3 phase 2.

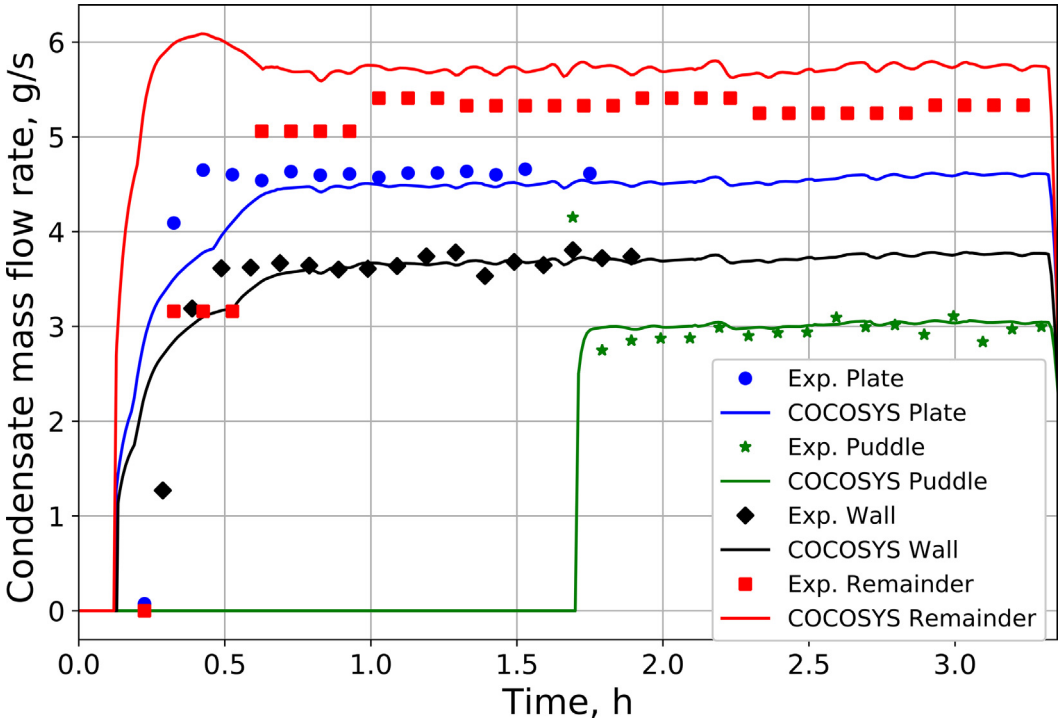

Fig. 5. Condensate mass flow rate comparison against THAI-AW3 phase 2.

the deviation of the condensation rate of the remainder section is not doubled to the plate section although the geometry is symmetric. The cooling power is different from section to section. The cooling system is the oil jacket around the containment vessel with cold oil inlet and heated oil outlet. The inhomogeneity could cause the wall heat flux differently. In addition, the fluctuation of steam injection, as shown in Fig. 1, leads to the fluctuation of the condensate flow rate. The condensate drained during the experiment from each test section is collected outside the vessel, which is measured manually every 45 sec once the drainage flow begins. The measured condensate of the puddle section is much later than the other three test sections since the condensate is reserved in the puddle for a long time (about 1.7 h) until the condensate overflows the weir of the puddle.

Taking into account the results presented in Fig. 4 and Fig. 5, the pressure and temperature in THAI-AW3 experiment are predicted well by COCOSYS and there are no significant differences between the calculation results and the measurement data. This compliance means the thermal-hydraulic model of COCOSYS is acceptable for further analysis on condensate coverage and aerosol wash-down process.

The cumulative aerosol wash-down masses of each section compared against the THAI-AW3 experiment are shown in Fig. 6. In the early beginning 1 h, aerosols are washed rapidly for all these three sections (wall, plate, and puddle; there is no wash-down experimental data of remainder section), then slowly in the later phase (after 1.5 h). The comparisons of aerosol wash-down generally show good agreements with experimental data, but still have deviations. The predictions of aerosol wash-down start a little earlier than the experiment since the rivulets occur before the measurement. The aerosol wash-down masses increase linearly in the later phase. An explanation is that the rivulet entrains the aerosol along rivulet edges. That means the rivulet could take the aerosols into water not only under the rivulet but also possibly from the two wedges of the rivulet. The rivulet entrainment is an additional source of the aerosol wash-down (Freitag et al., 2018). The wash-down from the puddle ground overestimated since the water reserved in the puddle may compact the aerosol for a while in reality before the water overflows the puddle weir, which leads to the increasing of aerosol critical shear stress. The final deviation of the wash-down mass at the end of experiment is possible that the uncertainty of rivulet coverage estimation has already about ±25% (Wang and Cheng, 2020).

Table 1 shows the aerosol wash-down mass comparison between the COCOSYS calculation and the THAI-AW3 experiment. The aerosol wash-down efficiency is defined as the ratio of aerosol wash-down mass to the total initially deposited aerosol mass. The experimental aerosol wash-down efficiency is about 16%, 9.5%, and 10.2% for the wall section, the plate section, and the puddle section respectively (Freitag et al., 2016). The total amount of aerosol collected in measurement is about 4.93 g for the wall section, in which 4.1 g aerosols are collected continuously for the first 1.5 h. The other aerosol removal is about 0.83 g during the later period. The corresponding vertical wall has 12.5 m^2 surface area with a total approximated load of 30.7 g; hence, approximately 16% of the silver aerosols have been removed during the whole wash-down phase. For the plate and puddle sections, the total mass load has to include the aerosol deposited on their corresponding trays (each section of 52 g). The aerosol wash-down efficiency calculated by COCOSYS is about 10%-14%. The predicted results are close to the experimental data.

3.4. Other analysis of interest

Fig. 7 reveals the condensate coverage (ε, as seen in Eq. (11)) distribution of different locations along the condensate streamwise. The condensate coverage in the plate section is taken as an example. The condensate coverage of each structure increases in the beginning and then keeps flat in the later phase. The result is consistent with the trend of the condensate mass flow rate, since the condensate Re number varies linearly with the condensate flow rate per width. Structures each have the same width. The lower

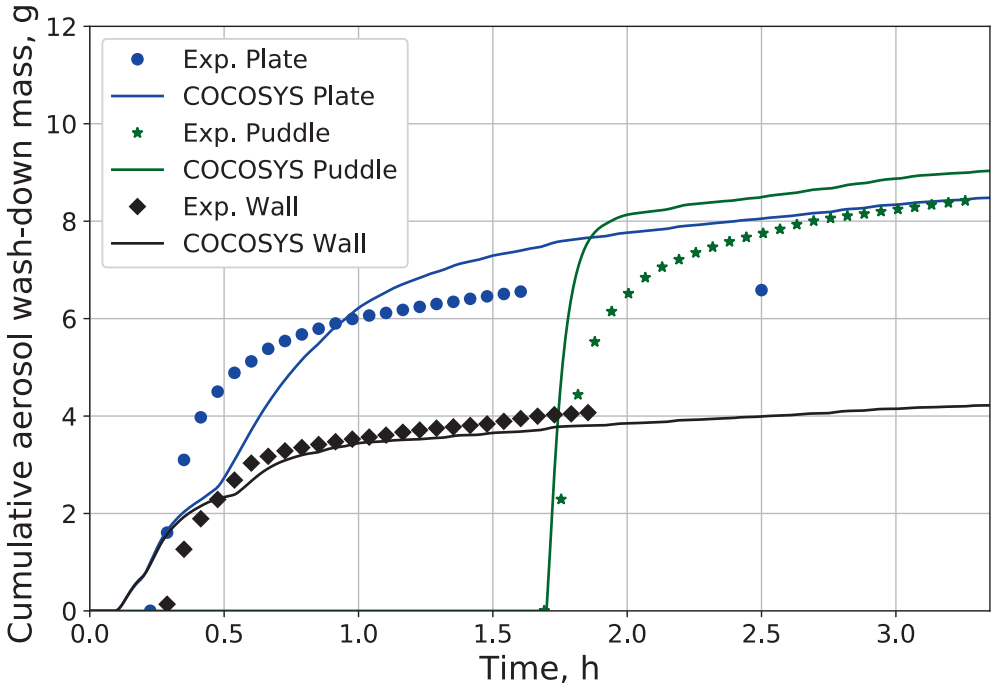

Fig. 6. Comparisons of aerosol wash-down mass of different test sections.

Table 1
Aerosol wash-down mass comparison.

	Wall section		Plate section		Puddle section	
	Exp.	Cal.	Exp.	Cal.	Exp.	Cal.
Total mass load, g	30.7(walls)		30.7(walls) + 52(tray)		30.7(walls) + 52(tray)	
Total mass wash-down, g	4.93	4.25	7.83	8.4	8.54	9.1
Efficiency	16%	13.8%	9.5%	10.1%	10.2%	11%

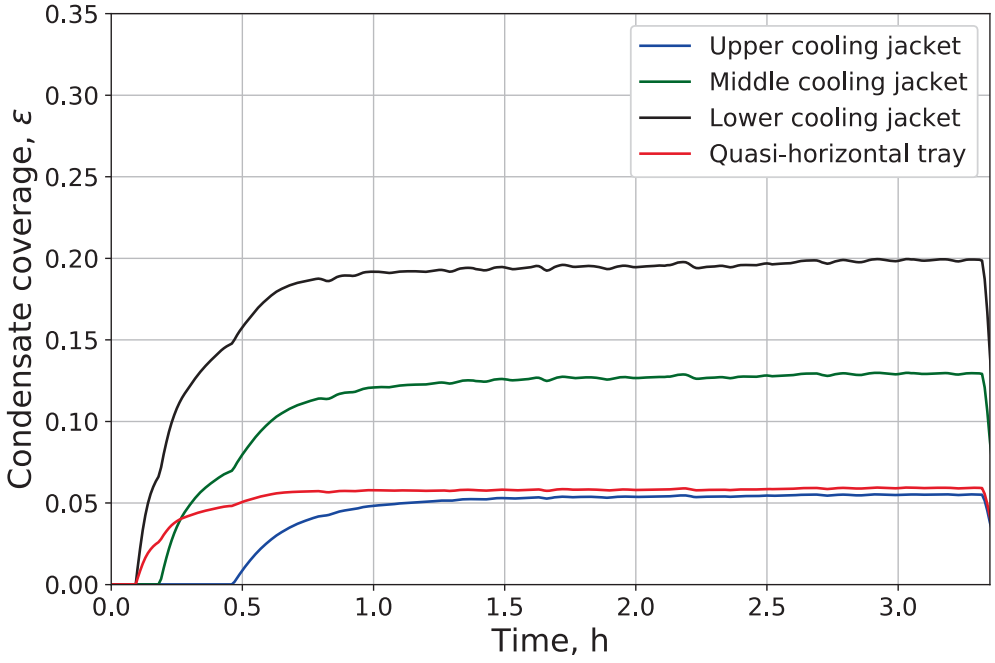

Fig. 7. Condensate coverage of different locations in plate section.

structure collects the upper stream flow, so that the water coverage of the lower structure is larger than the upper ones. Furthermore, there still are different onsets of the coverage evolution. For instance, the coverage of the lower cooling jacket structure starts in advance of the middle structure; similarly, the middle one is ahead of the upper one. That is because the temperature stratification occurs before condensation happens. The initial temperatures (namely the results at the end of phase 1 of the test) of structures are different (upper structure: 91 °C; middle: 80 °C; lower: 70 °C), which lead to the different onsets of condensation. The condensate coverage on quasi-horizontal trays is much less than the lower cooling jacket, mainly since the inclination angle changes from 90° to 2°. The condensate coverage decreases with the inclination angle reducing, as shown in the correlation Eq. (11).

The condensate coverage distribution influences the aerosol wash-down directly. The corresponding results of the cumulative aerosol wash-down mass of different locations in the plate section are shown in Fig. 8. The amount of aerosol wash-down is proportional to the magnitude of the condensate coverage. The onsets of the aerosol wash-down is exactly consistent with the condensate coverage as well as the onsets of condensation. The aerosol wash-down mass on the lower jacket is larger than the middle and upper ones, because the lower jacket has the entire condensate of vertical walls. However, the aerosol wash-down mass on the tray is higher than the vertical walls, although the tray has lower coverage. That is because the aerosol load 35.1 g/m^2 on the tray is about 14 times the load on vertical walls. The blue solid line in Fig. 8 is the total aerosol wash-down mass of the plate section, which is the summation of wash-down mass on vertical cooling jackets and the tray. The blue dashed line is the aerosol mass loading on total wetting area, which is the initial aerosol surface loading before condensation starts times the current wet surface that is calculated from condensate coverage ε. By comparing this aerosol mass load, the total aerosol wash-down mass is smaller in the beginning, but is almost the same in the latter phase. The gap between the blue solid and dashed lines is due to the aerosol wash-down process, which is such a decay function that it takes time to wash aerosols.

In summary, the simulation results are generally in good agreement with the experimental data. The key-lessons learned from the validation exercise possibly used in application activities are: (1) The condensate coverage crucially influences the aerosol wash-down efficiency. Thus, a reliable model such as the newly developed model CONRAG is necessary to be implemented into the COCOSYS code, instead of a user-defined value. (2) The constants used in the aerosol wash-down model are defined here by experiment result, e.g., the aerosol effective density is 1550 kg/m^3 due to the steam condensed on the aerosol surface. The erosion constant is 0.03 1/s, which is, however, dependent on the aerosol particle properties. (3) The nodalisation and heat transfer model should be acceptable for the simulation of the containment thermal hydraulics. However, the further integral validation against an experiment with deposition and wash-down processes occurring at the same time, are still of interest.

4. Analysis of aerosol wash-down in generic containment

The purpose of this chapter is to test and apply the aerosol wash-down model coupled with condensate coverage correlation in a generic containment. It is to check out how the severe accident scenario affect the aerosol behavior, e.g. the aerosol injection, deposition, wash-down, distribution, etc. To be sure, here the aerosol wash-down phenomenon is emphasized.

4.1. COCOSYS model of generic containment

The general specification of the generic containment is referred to a German pressurized water reactor (PWR) with 1300 MWe (Bönigke et al., 1998). The reactor system consists of four primary coolant loops with vertical U-tube steam generators. The reactor cooling systems (including steam generators, pumps, etc.) are located in equipment compartments separately. Containment is subdivided into several compartments. In case of the overpressure in the compartments, the rupture discs will open to enable atmospheric flow to the neighboring compartments or the dome ulti-

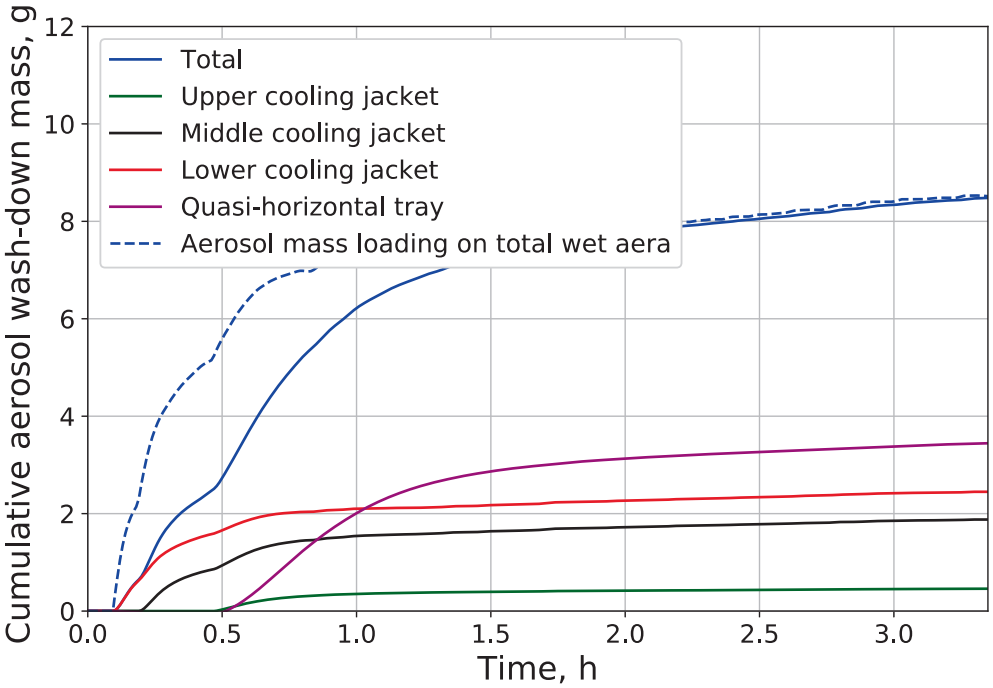

Fig. 8. Cumulative aerosol wash-down mass of different locations in plate section.

mately. The reactor building consists of an inner steel shell of design pressure 8 bar and volume 70000 m^3, which contains the reactor system, as well as an outer concrete building, which houses the safeguard compartments of volume 42000 m^3 (Kelm et al., 2014). The containment provides a barrier against the release of radioactive fission products.

- Nodalisation

Within the European SARNET2 project (Severe Accident Research NETwork of excellence), a 'Generic Containment' nodalisation, based on this German PWR, was defined in order to investigate the influence of user effect, LP containment code, and modeling choice on the calculation results of a nuclear power plant scale. It was used to compare and evaluate the analyses performed with different LP codes and models as a benchmark exercise. This 'Generic Containment' was applied for testing new models on plant scale (Kelm et al., 2014, for testing the hydrogen recombiner models) and performing the uncertainty and sensitivity analysis (Povilaitis et al., 2017).

The benchmark was composed of three exercise runs with increasing complexity: Run-0, Run-1, and Run-2. 'Run-0′ concerned only the containment thermal-hydraulics of the in-vessel phase during a small break loss-of-coolant accident (SB-LOCA). The main objectives of Run-0 with the comparison of obtained results, were to develop the comparable inputdecks for different codes and to evaluate the modellings. While 'Run-0′ was conducted as an initial preparatory step, the 'Run-1′ (Kelm et al., 2013) is extended for severe accidents by including releases of H_2, CO and CO_2 in-vessel and ex-vessel. The subsequent 'Run-2′ was additionally extended by adding a system of passive autocatalytic recombiners (PAR) in order to test different PAR modelling approaches (Kelm et al., 2014).

The original nodalisation of the benchmark was developed by Forschungszentrum Jülich (FZJ) and RWTH Aachen University (RWTH) for the SARNET2 Generic Containment activity (Kelm et al., 2014). In this paper the containment dome is refined into several layers, specified the water flow path on containment shell structures, the structure inclination angle, and contact angle for the simulation of aerosol wash-down. Fig. 9 gives an overview of the refined control volumes and the connections between them.

The compartments of the reactor and auxiliary building have been grouped in 34 control volumes (zones) in the generic containment nodalisation. In addition, the real structures and flow paths have been merged in order to reduce the model complexity. The four loops have been grouped. Therefore, there are two steam generator compartments R-SG12 and R-SG34 as well as the corresponding annular compartments behind the cylindrical shield R-ANN12 and R-ANN34, which are associated with the U-12 and U-34 as the safeguard compartments. There is a common sump zone R-SUMP within the safeguard building (U) U-SUMP. The reactor cavity R-CAVITY as well as the pipe duct room R-DUCT is represented by a single zone respectively. There is a connection from the containment to the safeguard building in order to consider the design leakage. Gas distributed in the two compartments of nuclear auxiliary building (AB) AB-UP1 & 2, can be vented by the exhaust chimney AB-CHIM to the surrounding environment ENVIRON.

COCOSYS analysis on THAI-AW3 experiment reveals the condensate coverage on the containment shell increases along the condensate flow streamwise on structures. Therefore, in order to investigate the condensate coverage distribution, the dome zone R-DOME is refined into ten layers (from bottom zone R-DOME01 to top zone R-DOME10), as shown in Fig. 9. These ten layers of dome are within the corresponding ten safeguard building zones (from bottom zone U-DOME01 to top zone U-DOME10).

All zones are connected by using single atmospheric (gas) and drain (liquid) junctions. For simulating the water flow along the containment shell, the flow paths are defined in a specific way, such as the condensate flow from the upper structures to the lower structures in the neighboring zones. In order to reduce complexity, doors, rupture discs, and pressure relief flaps are merged and considered in a simple way by using rupture disc models. The total heat capacity and the heat transfer area have been preserved. In order to have a common representation, especially of the total heat capacities, the properties of concrete and steel are defined (Kelm et al., 2014). Each zone below the dome contains vertical and horizontal both steel and concrete structures, which represent the overall heat exchange surface located in each zone. However, for the containment shell structures, the inclination angle increases step-by-step from top structure in zone R-DOME10 with 15° to bottom one in R-DOME01 with 90°. In order to keep consistent with the aerosol wash-down model, some heat structure parameters, such as the contact angle, characteristic length and height, condensation model, etc., have to be specified. Compared with the benchmark Run-1, two additional atmosphere junctions are added to connect the zone U-DOME01 and U-DOME10 to the environment, so that the containment shell is specified as the containment long term cooling system. All other structures are considered as heat reservoirs. Both wall-gas-wall and wall-gas radiative heat exchanges (so called 'WWR' and 'WGR' in COCOSYS) are considered in the simulation. However, the view factors are default for the radiations, which is calculated automatically depending on the zone definition and the heat structure area.

- Hypothetical accident scenario

A small break cross section of 50 cm^2 SB-LOCA with the loss of secondary heat sink and all active safety injection systems are simulated by using the specified source term injections. The location of the pipe break is on the connecting line of the safety injection system, where the injection of one accumulator releases directly to the sump. The source terms representing the release from the primary circuit and later MCCI are defined in the sump zone and reactor cavity zone respectively. The releases of steam, liquid water, hydrogen during in-vessel phase and hydrogen, carbon monoxide and dioxide during ex-vessel phase are modelled by using the source terms in the form as pre-calculated tables. Energy source terms are also given and used to account for the fission product decay heat, heat losses (e.g. from the RPV), heat emission of the core melt, etc.

The events of the accident scenario are the same as generic containment benchmark Run-1, except the aerosol injection at 2040 sec. The simulated accident scenario is summarized in Table 2.

At 1800 sec after the blow-down phase, the reactor core heat-up begins. Hydrogen and aerosol start to release in a subsequent few minutes due to the core degradation. At 3000 sec, the hot leg accumulators start water injection and lead to a reflooding of the damaged core. After vaporization of the water and pressure decrease in the primary circuit, the remaining water of the accumulators is injected at 8000 sec. With the core damage continuing, the core melt relocates to the lower plenum of the RPV at 11,200 sec. At 12,280 sec, the RPV fails and the core melt relocates to the reactor cavity. The SB-LOCA is extended to a full severe accident transient including H_2, CO, and CO_2 release during ex-vessel phase.

The parameters required in aerosol wash-down model, such as the equilibrium contact angle, the effective particle density, and the erosion constant, etc., are set as the same as in THAI-AW3 COCOSYS simulation. However, the aerosol surface load on each individual surface should not be initialized; instead, the aerosol injection has to be activated. The calculation of the aerosol surface

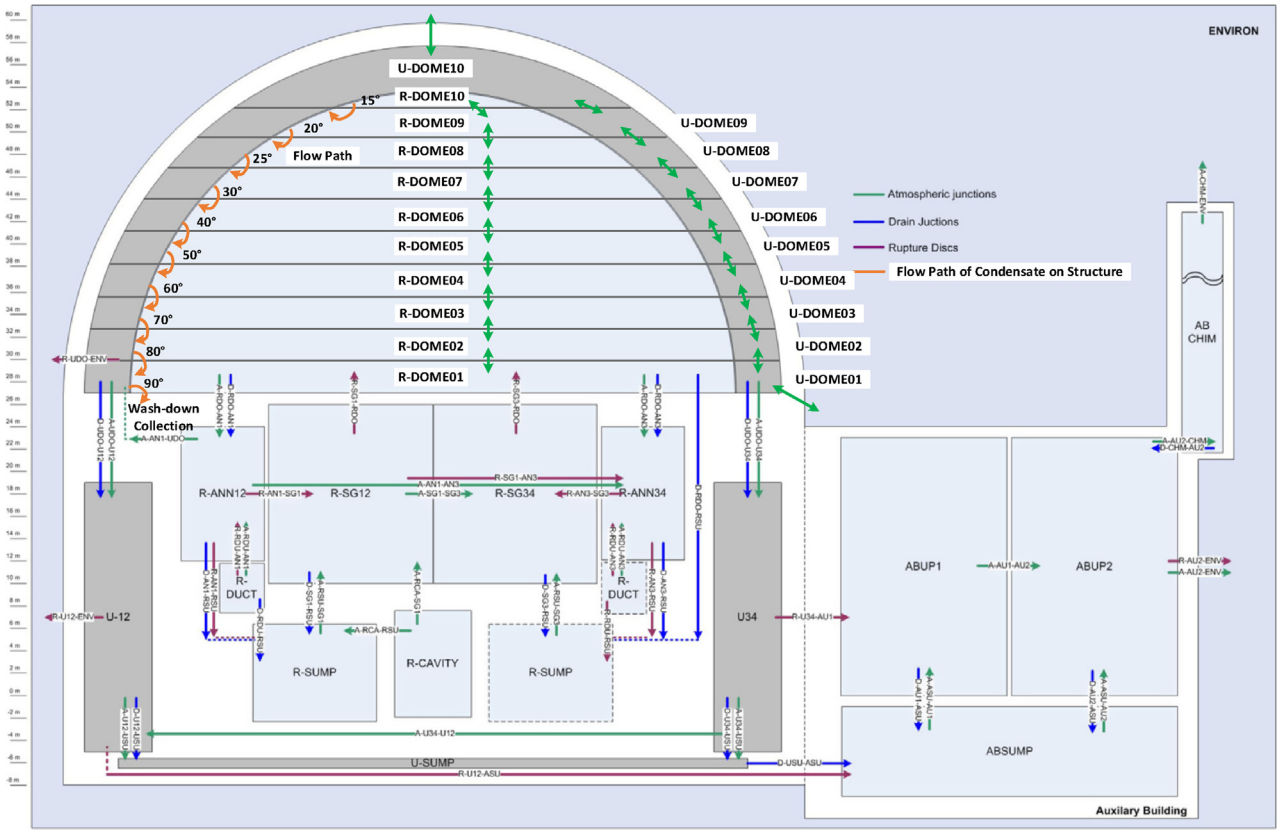

Fig. 9. Generic containment nodalisation refined on the basis of (Kelm et al., 2014).

Table 2
Extended SB-LOCA accident scenario.

Time, sec	Event
0	Break and blow-down happen
1800	Beginning of core heat-up and degradation
2040	Aerosol release
3000	Injection of hot leg accumulators
11,200	Lower plenum core melt relocation
12,280	RPV failure & melt relocation to the cavity
>12280	Molten Core-Concrete Interaction
46,800	End of the simulated transient

density on walls is the contribution of the aerosol deposition model in COCOSYS.

The aerosol injects after the core degradation, which has a similar trend of hydrogen injection (Sangiorgi et al., 2015). The insoluble aerosol injection rate, kg/s, is valuated proportionally to the hydrogen injection rate with the total accumulated amount about 1000 kg insoluble aerosols of a German Konvoi containment (Weber, 2011), as shown in Fig. 10. During the in-vessel phase, about 345 kg of insoluble aerosols is released from core damage and relocation. And then during the ex-vessel phase a continuous term is released from MCCI with a very stable aerosol injection rate. The cumulative aerosol injection mass increases quickly twice in the in-vessel phase due to the core degradation and core melt relocation respectively, and then increases linearly during the ex-vessel phase. The insoluble aerosol Ag is simulated currently, whose properties are the same as the Ag in THAI experiment simulation. The shape and size of aerosols influences the wash-down process, since the aerosol diameter and porosity determine the cohesive force between particles. The corespongding sensitivity analysis (Wang and Cheng, 2020) conludes that the smaller diameter and porosity leads to a lager cohesion decreasing the aerosol wash-down efficiency. The mass-median-diameter is about 1.1 μm with log-normal size distribution. The effective density is 1550 kg/m^3, the erosion constant $k_{e,0} = 0.03$ and the equilibrium contact angle is 14°.

Actually there are soluble aerosols injected during severe accidents, e.g. around 250 kg of German Konvoi containment (Weber, 2011). The soluble aerosols, like CsI, are unneglectable from the perspective of the quantity of fission products. THAI-AW2 has been performed to investigate the wash-down behavior of soluble CsI and insoluble SnO_2 aerosol mixture. The experimental results concluded the wash-down efficiencies were independent from the soluble CsI and insoluble SnO_2 aerosols each other. The aerosol wash-down behavior was that the time range of aerosol wash-down was from minutes to hours and the completeness of aerosol wash-down was dependent on the water flow, the aerosol surface load, and the surface characteristics (Gupta et al., 2012). The soluble aerosols are quickly dissolved and transported with the condensate flow. The dissolution process can be simplified as an instantaneous (perhaps to be improved as time-dependent) and complete dissolution of wetted particles in COCOSYS. The wash-down of insoluble aerosols however remained far from being complete. The AULA - model is developed for the wash-down of insoluble aerosols. In addition, the CONRAG is only coupled within the AULA so far. Therefore, the wash-down of soluble aerosols are not simulated in the current application.

In COCOSYS, the modeling of aerosol dynamics, e.g. the agglomeration and deposition of aerosol particles, are done by using the MAEROS model, which is one of the earliest models to use the sectional method for the prediction of aerosol behavior in a control volume, and is both multi-sectional and multi-component. The types of aerosols can be defined in the input deck by means of size

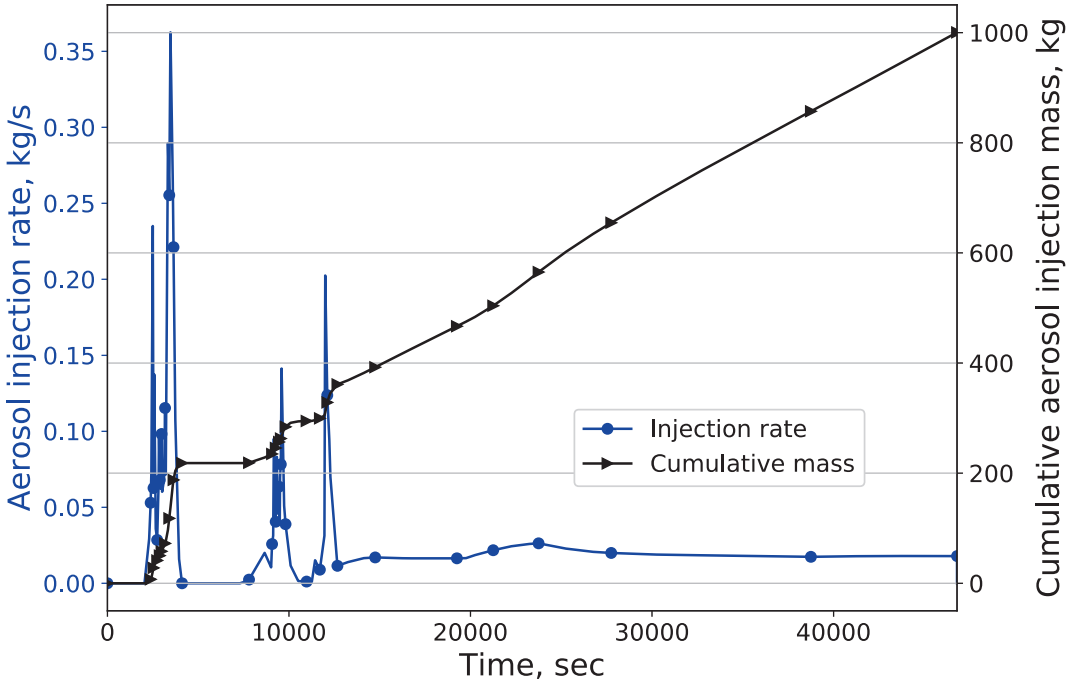

Fig. 10. Insoluble aerosol injection.

distribution, density, erosion constant, and so on. The modeling of aerosol dynamics can be combined with the MGA (moving-grid method) condensation model considering the particle growth and shrinking rate. During the condensation interval, the thermal–hydraulic boundary conditions remain constant. They are only updated before the next interval. In the aerosol interval with MAEROS that follows, the 'wet' aerosol is treated like a 'dry' one. Agglomeration and deposition of the droplets are calculated as if they were solid particles (Klein-Heßling et al., 2015).

The decay heat of fission products is considered in a simple way by means of energy source terms in each zone. The combustion of burnable gas mixtures, PAR system, and containment spray system are not considered in the current run. The calculations are performed for a period of 46,800 sec in order to investigate the containment thermal-hydraulics and aerosol wash-down process under a full severe accident transient.

4.2. Thermal-hydraulic results

Fig. 11 shows the trends of the generic containment pressure and temperature during the full severe accident scenario transient. The results predict three pressure peaks. The first two peaks are related to the blow-down and hot leg accumulator injections at those two moments. The quenching during core melt relocation to the RPV lower head causes the third pressure peak. The pressure evolution before RPV failure is comparable to the benchmark results, possibly due to the nodelization refinement and the modification of heat structure definition. After the RPV failure, although the fission product decay heat, steam, and no-condensable gas are still released into the containment because of MCCI, the containment long term cooling system has already activated to cool the containment down, resulting the pressure less than the benchmark Run-1 (blue dashed line, no air from the environment flows through the gap of containment). The comparison generally proves that the implementation of the 'Generic Containment' is comparable to the one developed within SARNET2 activity and acceptable to continue the further studies. The average temperatures of gas in the dome and on the inner surface of the containment shell have similar trends of pressure, as also shown in Fig. 11. The important steam sinks are the condensation on walls and sumps in the beginning. From the green solid line in Fig. 11, it can be seen that there is a large amount of steam released in the containment during the blow-down phase. Therefore, the pressure (blue solid line) and temperatures (black lines) increase rapidly in the beginning. Comparing the steam mass flow rate in the containment, the trend observed is quite similar to the pressure, which shows the pressure level is corresponding to the steam mass flow.

Fig. 12 shows the condensate mass flow rate per width on the containment shell. The structures over the elevation linking zones R-DOME01, 03, 05, 07, and 09 are taken as examples. During the blow-down phase, the condensate mass flow rate per width of each structure has a peak above 0.01 kg/(m·s), and then the value goes down to zero quickly since there is no steam release into containment at that moment. The mass flow rate per width recovers and gets several peaks later because of the steam injections again. After the RPV failure, the condensate mass flow rate per width increases gradually to a stable level. As discussed on the condensate of THAI-AW3 experiment before, the lower structure collects the condensate from the upper structures. Therefore, the lowest structure linking zone R-DOME01 has the largest condensate mass flow rate.

Consequently, in Fig. 13, the condensate coverage ε on the inner surface of the containment shell has an identical trend as the condensate mass flow rate per width. The results show condensate flow dominates the condensate coverage in the current run. Because the contact angles of the structures of containment shell are defined as the same, the *Ka* numbers of the condensate are similar since *Ka* is temperature dependent (see the temperature in Fig. 11), and the inclination angle also does not change the coverage much once the angle larger than 30°. Therefore, according to the correlation of condensate coverage Eq. (11), Re number, in other words the condensate mass flow rate per width in current run, dominates the water coverage. Fig. 13 reveals additionally the coverage of most structures of the containment shell is not over 20% in the long-term phase. The surface is 100% covered by condensate if its mass flow rate per width is above 0.01 kg/(m·s).

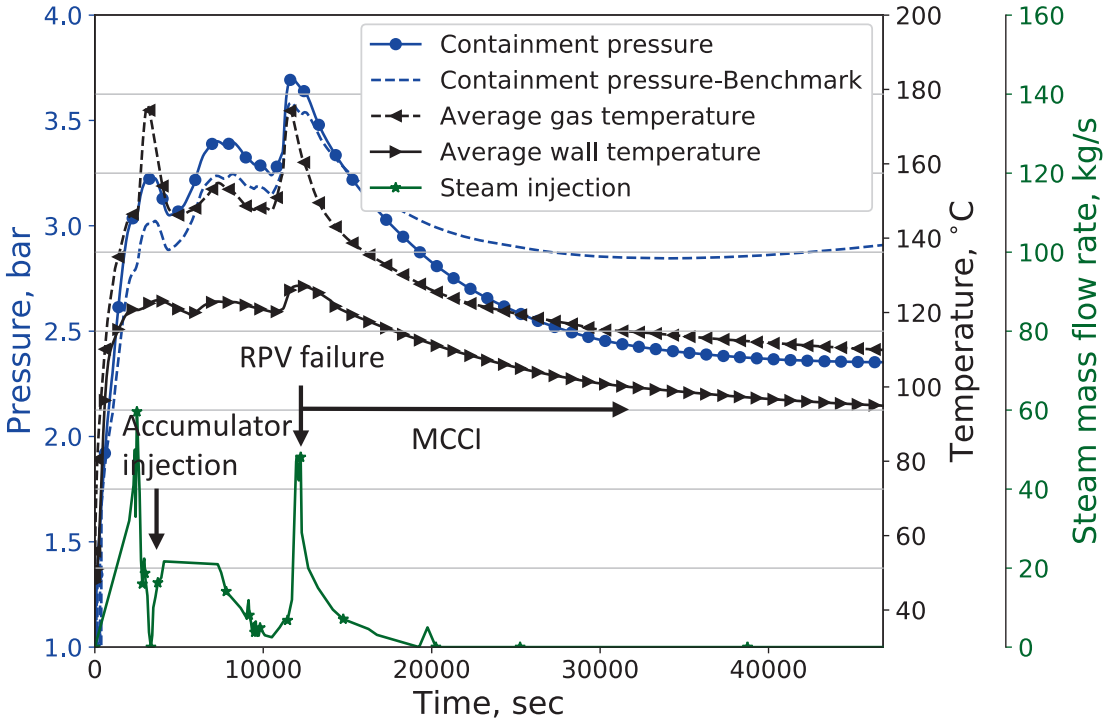

Fig. 11. Generic containment pressure and temperature evolutions.

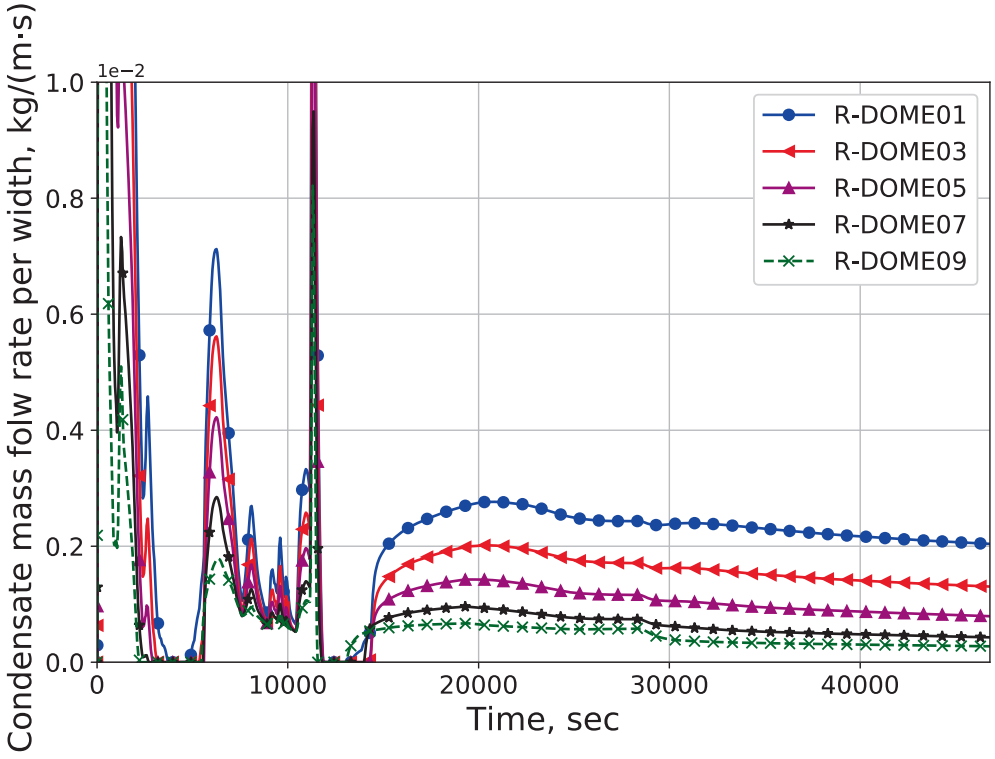

Fig. 12. Condensate mass flow rate per width on containment shell.

4.3. Aerosol wash-down

Fig. 14 presents the airborne aerosol concentration of the Ag component in the containment atmosphere. There are three peaks of aerosol concentration in the containment atmosphere during its evolution, which are consistent exactly with the trend of aerosol injection, as seen in Fig. 10. During the ex-vessel phase, the concentration keeps stable as well as the aerosol injection rate stays constant. The aerosol injects in the zone R-SUMP, then the aerosols are carried by the gas flows to the neighboring zones, e.g. the cavity, the pipe duct room, and two SG compartments. Some of the aerosols deposit on there, some of them are continuously taken

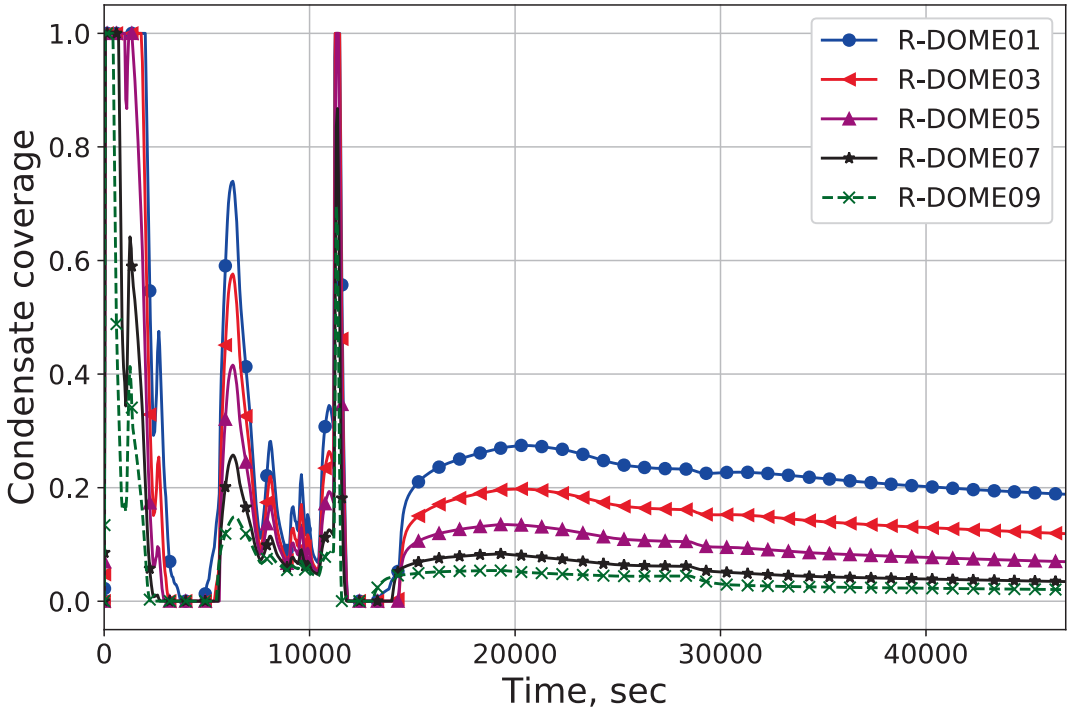

Fig. 13. Condensate coverage on the inner surface of containment shell.

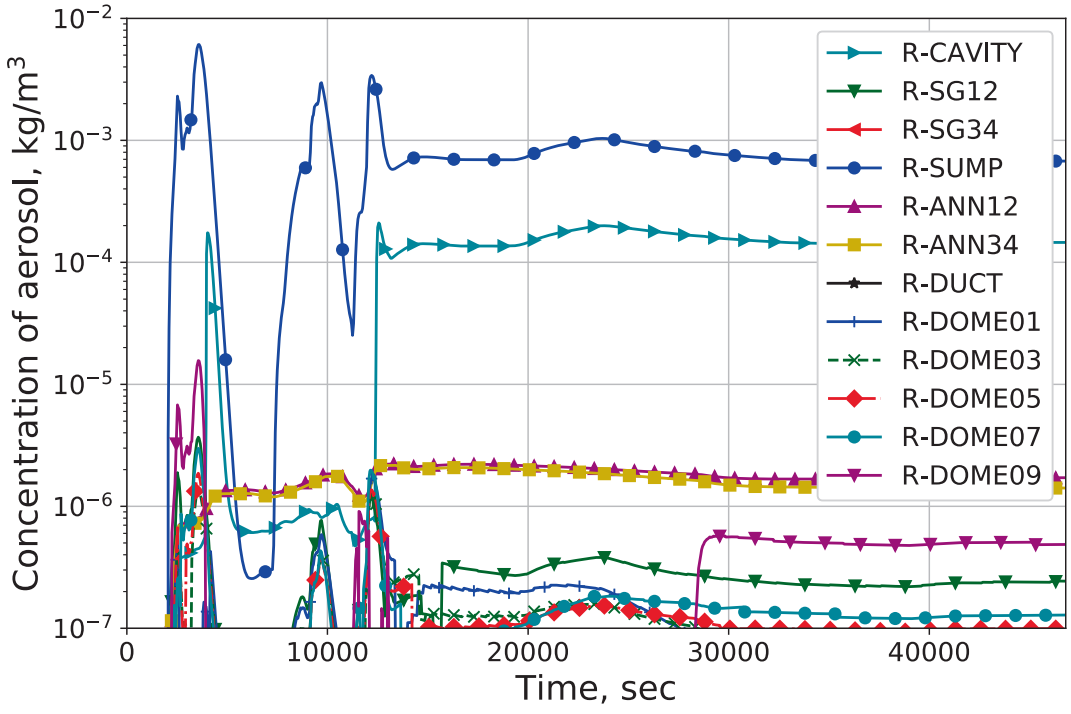

Fig. 14. Concentration evolution of airborne aerosol inside containment.

by the gas flow to next surrounding rooms, and transported into the containment dome. During the ex-vessel phase, there are three aerosol concentration groups. The concentrations of sump and cavity are about 10^{-3}–10^{-4} kg/m^3. The concentration of the annular compartments under the dome is about 10^{-6} kg/m^3. The last group is the concentration in dome, SG and pipe duct compartments, in which the concentration is about below 10^{-6} kg/m^3. The aerosol concentration in dome is much less than in sump and cavity, since the dome is far away from the aerosol release location and the condensation effect on the containment shell enhances the deposition of the aerosol in the atmosphere.

Fig. 15 reveals the aerosol wash-down rate (blue solid line) and the accumulated aerosol wash-down mass (black solid line) over the full severe accident transient. The aerosol wash-down activates after aerosol injection and the condensate covers the structure after the blow-down. The aerosol wash-down rate fluctuates until

the accident goes into the ex-vessel phase, then it maintains at a low level about 0.003 kg/s. As a consequence, the cumulative aerosol wash-down mass increases fast before the RPV failure and then linearly in the later phase. There are about 173.65 kg aerosols on the containment shell washed down by condensate flow. The black dashed line in Fig. 15 shows the quantity of the total deposited aerosol mass on the containment shell over time. The gap between aerosol mass deposited on containment shell and the aerosol wash-down mass (black solid line) is moderate during the in-vessel phase, but becomes larger during the ex-vessel phase. The evolution of aerosol wash-down efficiency (the green solid line) goes up before the RPV failure, then goes down to nearly 30% at the end of the accident transient. That means it is close to 30% aerosols (mass) deposited on the containment shell are washed down to the condensate sump at the end. The trend of aerosol wash-down efficiency is strongly coupled with the condensate coverage. E.g. during the in-vessel phase, the efficiency increasing rapidly twice is corresponding with the two peaks of condensate coverage. The aerosol wash-down efficiency decreases during the ex-vessel phase since the average condensate coverage is less than before.

Fig. 16 presents the aerosol distribution inside containment over time. COCOSYS can offer the results of aerosol concentration, deposition, wash-down of each zone or structure. Here, the aerosol distributions are grouped into three parts: airborne aerosol mass (the aerosol in all zones atmosphere), aerosol mass remained on the containment shell, and others aerosol mass (mainly on structures and in sumps under the dome). Based on the aerosol concentration in zones are known, the evolution of the airborne aerosol mass suspending in the containment atmosphere over the whole accident scenario can be computed, which is about 4 kg at the end but has a peak value around 20 kg, as seen in the green line in Fig. 16. Compared to the total amount of aerosol injected into containment, 1000 kg, there is only 0.4% of aerosols suspending in the containment atmosphere. That is to say 99.6% of aerosols is deposited on walls and relocated in sumps due to the aerosol transport. The aerosol mass remained on the containment shell, as shown in the black solid line, equals the deposited mass on the containment shell minus the wash-down mass. The retention of aerosol on structures and in sumps under the containment dome including the aerosol wash-down mass, is about 531 kg at the end, as seen in the blue line. That means 53.1% of aerosols reserves under the containment dome, 46.5% remains on the containment shell inner surface, and 0.4% suspends in the containment atmosphere. The aerosol mass transported to the water sump via wash-down in comparison to the direct sedimentation of aerosols in the sump can be also approximated. E.g., at the end of the current case, the direct sedimentation of aerosols on the water sump is about 357.35 kg. Therefore, the ratio of the aerosol wash-down mass to the direct sedimentation is about 0.486.

In a short, aerosol wash-down is one of the key factors to distribute the aerosols in nuclear containment. Actually, the aerosol distribution over time is dependent on the severe accident scenario. In the current run, the containment spray system is not designed for instance, since there is no spray system installed in this German PWR containment (but e.g. installed in other PWRs like French EPR). Experiments and simulations tell the water spray inside containment can remove the airborne aerosol in the atmosphere during severe accidents (Allelein et al., 2009). The containment spray may reduce the aerosol amount deposited on the containment shell, which leads to the decrease of aerosol wash-down mass.

Fig. 17 presents the comparison of aerosol wash-down results calculated by the current modified COCOSYS and the previous COCOSYS version (without coupling CONRAG model). The condensate coverage ε in the previous COCOSYS is user-defined. Here the condensate coverage is set as 50% for each structure in the containment, which is taken as an example for the following discussion. In the calculation of previous COCOSYS, there are about 96.2 kg aerosols on the containment shell washed down by condensate flow, which is much less than the modified COCOSYS result of 173.65 kg. Not only for the ultimate results of aerosol wash-down but also for their evolutions, there are big gaps between these two calculations. The evolution of the total aerosol wash-down efficiency has similar comparison conclusions of aerosol wash-down mass. In the calculation of coverage 50%, a lot of the

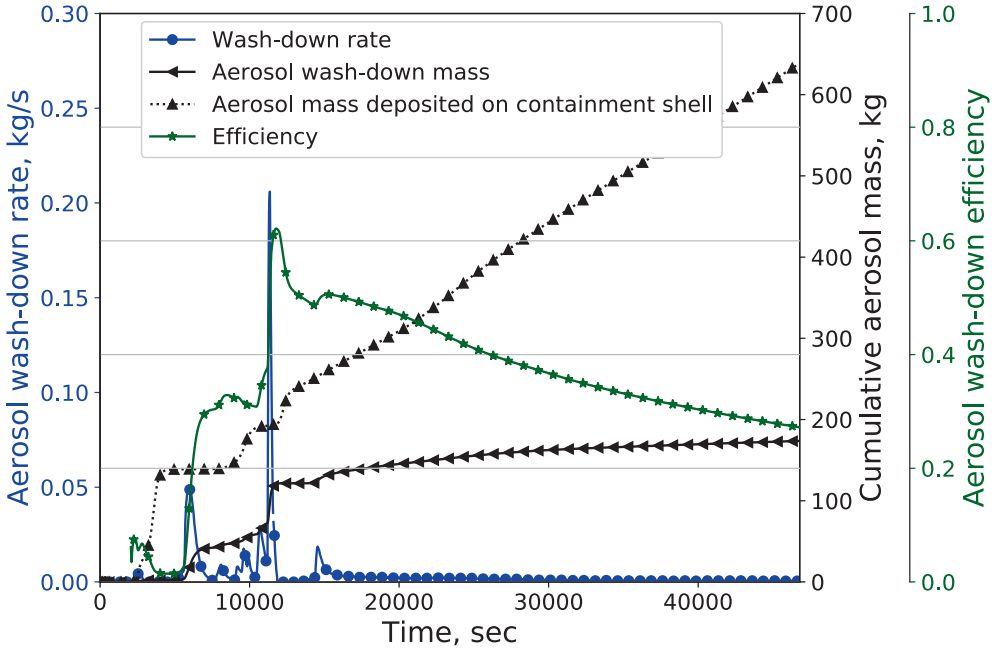

Fig. 15. Aerosol wash-down results.

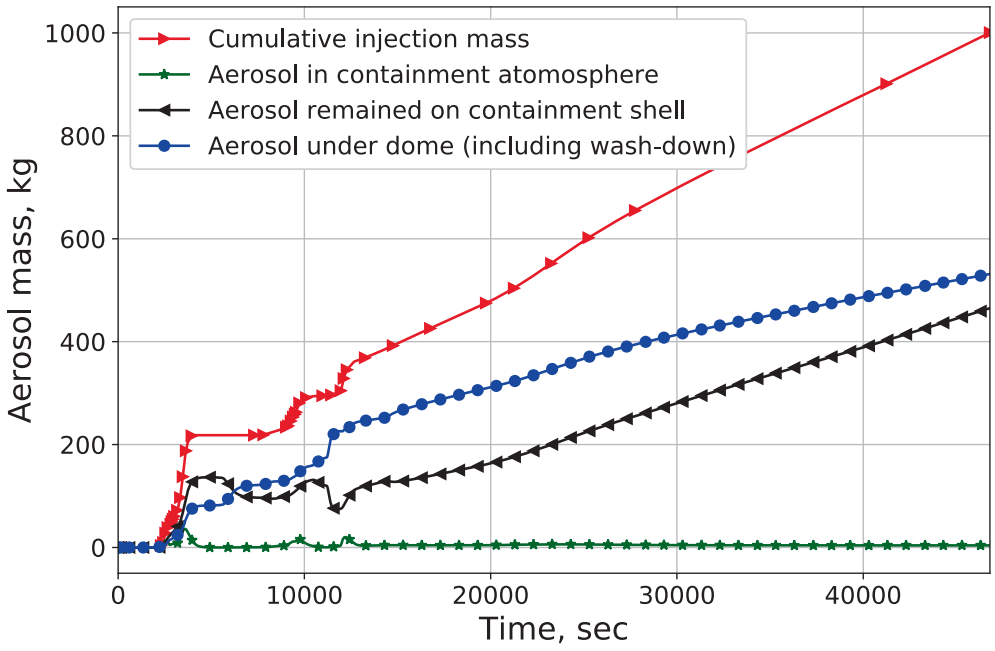

Fig. 16. Aerosol distribution over time.

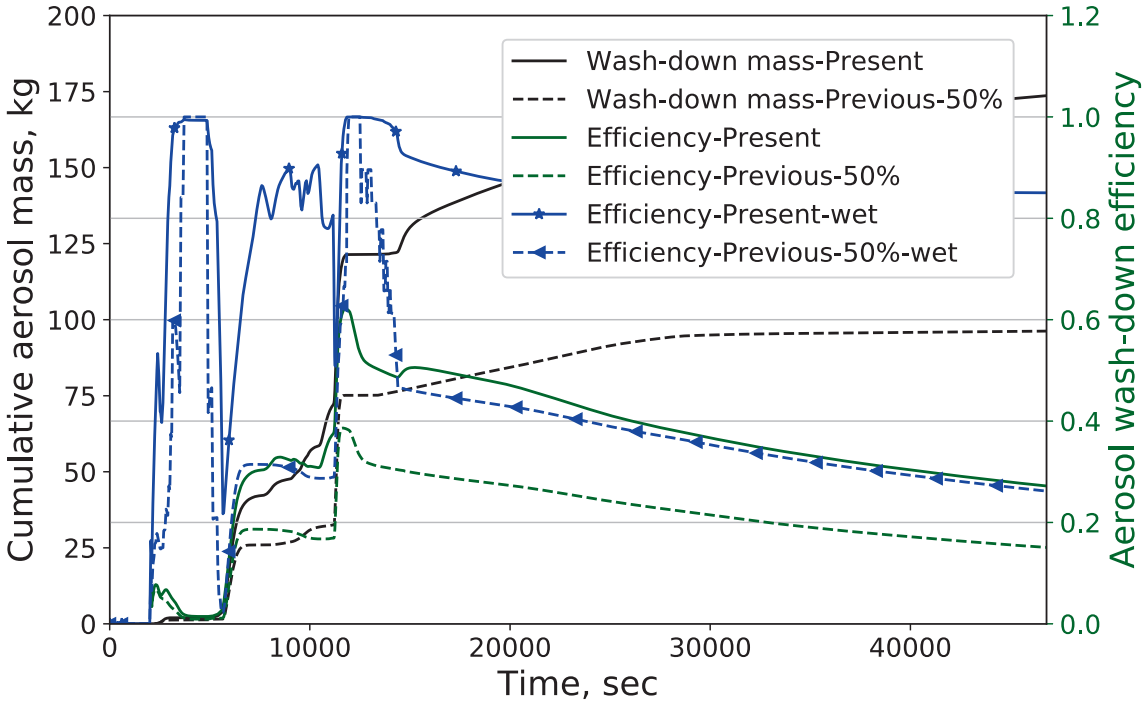

Fig. 17. Comparison of aerosol wash-down results.

deposited aerosol is not washed-down in contrast to the calculation with CONRAG, although the condensate coverage is smaller than 50%.

However, it is wondering that the higher condensate coverage 50% on the containment shell, compared with the calculation of the modified COCOSYS (see Fig. 13, less than 20% of most structures in most of the time), involves a lower aerosol wash-down efficiency. That is because it has to be considered if the condensate coverage is effective for the aerosol wash-down process. Two blue lines in Fig. 17 present the aerosol wash-down efficiencies on the wet parts of the surfaces (indicated with "wet" in legend of Fig. 17), which indicate a large deviation between them. It is one main objective of the CONRAG model shown in this containment analysis.

Fig. 18 shows the comparison of aerosol erosion rate of the structure in zone R-DOME01. The black dashed line of the coverage defined by 50%, has several higher periods of aerosol wash-down during the in-vessel phase, since the coverage is more than 50% in the calculation of the modified COCOSYS, as shown in Fig. 13. The larger coverage leads to the smaller condensate velocity due to the mass conservation. With the similar reason, during the ex-vessel phase, the condensate volume flow rate drops a lot while

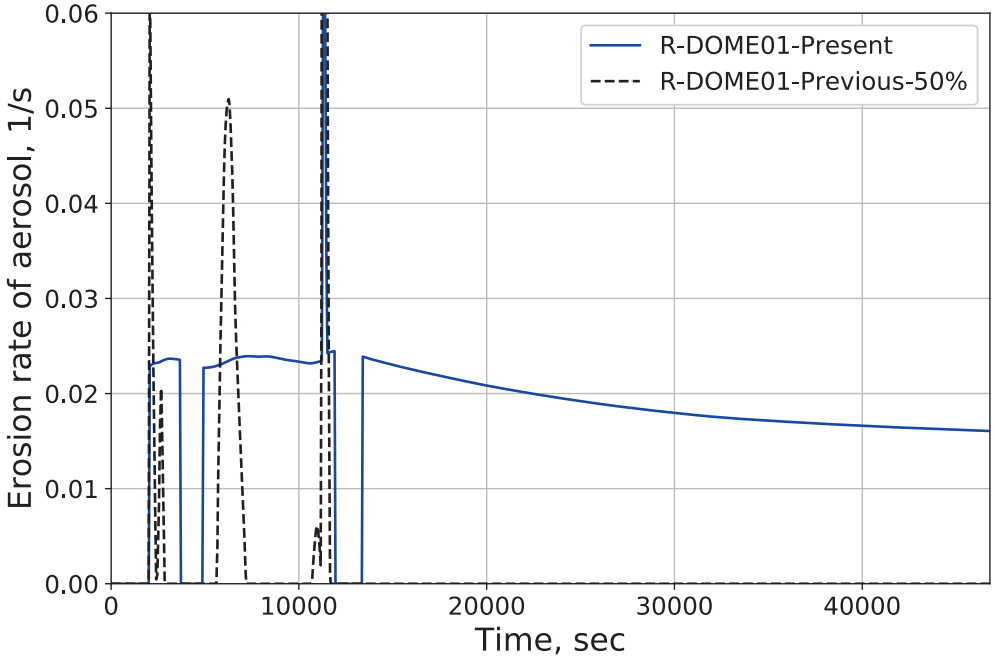

Fig. 18. Comparison of aerosol erosion rate.

the coverage keeps 50%, which leads to the condensate velocity is so smaller that its shear velocity is below the critical for aerosol wash-down. That results in the erosion rate during the ex-vessel phase is zero while it is positive in calculation of the modified COCOSYS. Therefore, it is hard to conclude a user-defined coverage is whether conservative or non-conservative. If the shear stress of condensate flow exceeds the critical, the smaller user-defined coverage deserves smaller wash-down mass.

5. Conclusions

The aerosol wash-down process is significant to evaluate radioactive source term distribution in nuclear containment. The work presented aims at validating and evaluating the newly modified aerosol wash-down model AULA coupled with condensate coverage model CONRAG in COCOSYS. This modified COCOSYS is used to simulate the THAI-AW3 integral experiment and the generic containment.

The validation against THAI-AW3 experiment is presented. Firstly, the containment thermal-hydraulics, such as the containment pressure, temperature, and condensation on structures are predicted well, which means the thermal-hydraulic model of COCOSYS is acceptable to enable further analysis on aerosol wash-down process. Secondly, the condensate coverage evolution is consistent with the trend of the condensate mass flow rate per width. The lower structure collecting the upper stream flow has a larger water coverage than the upper one. Lastly, the estimation of the condensate coverage is a necessary boundary condition for calculating aerosol wash-down. The aerosol wash-down mass is proportional to the magnitude of the amount of condensate coverage. The aerosols are washed down rapidly in the beginning, but slowly in the later phase. There are no significant differences of aerosol wash-down efficiency between the calculation and measurement. The key-lessons learned from the validation exercise are the activation of the condensate coverage model, the careful definition of heat structures, the experiment-dependent constants for aerosol wash-down, and the acceptable nodalisation and heat transfer model for thermal-hydraulics.

The 'Generic Containment' developed within the European SARNET2 project is referred to evaluate the applicability of the modified aerosol wash-down model and to investigate the severe accident scenario effect on aerosol wash-down behavior. The original nodalisation is refined (e.g. the containment dome is subdivided into ten layers) and modified (e.g. the water flow paths, inclinations, and contact angles of containment shell structures are specified in order to be consistent with aerosol wash-down process). The insoluble aerosol injection rate is assumed proportionally to the hydrogen with an accumulated amount 1000 kg. The evolutions of thermal-hydraulic parameters in the generic containment during the pre-defined severe accident scenario, are corresponding to source term injections (e.g. steam and energy). The condensate coverage on the inner surface of the containment shell has an identical trend as the condensate mass flow rate per width. The concentration of aerosol in the containment atmosphere is consistent with the aerosol injection, and dependent on the gas flow from the aerosol release location and the condensation effect of cold structures. The trend of the aerosol wash-down efficiency over time is strongly coupled with the condensate coverage. The comparison with the previous COCOSYS simulation reveals that the calculated results are quite different from each other. The higher coverage defined by the user could lead to lower aerosol wash-down efficiency due to the lower shear velocity. It concludes that the modification of COCOSYS, e.g. the coupling with condensate coverage model CONRAG, is necessary to investigate the aerosol wash-down process.

Concerning the further model developments and validations, for instance, the influence of the condensate coverage model on heat transfer, the integral validation against an experiment with deposition and wash-down processes occurring at the same time, are still of great interest.

CRediT authorship contribution statement

Fangnian Wang: Conceptualization, Writing - original draft. **Xu Cheng:** Supervision, Writing - review & editing. **Sanjeev Gupta:** Data curation, writing - review & editing.

Declaration of Competing Interest

The authors declare that they have no known competing financial interests or personal relationships that could have appeared to influence the work reported in this paper.

Acknowledgments

This work is supported by the project "Erweiterung des Strömungsmodells zur Simulation des Aerosolabwaschens (ESSA, grant number: 1501537)" and "THAI-AW3 experiment conducted as part of the THAI-V national programme (Project number 1501455), funded by the German Federal Ministry for Economic Affairs and Energy (BMWi), on the basis of a decision of the German Bundestag. We thank our partners Holger Norwack, Sara Beck from GRS. I also thank the financial support from China Scholarship Council (CSC, China, File Number: 201709110142).

Reference

Allelein, H. J., et al., 2009. State-of-the-art report on nuclear aerosols. OECD NEA/CSNI/R (2009) 5.

Amend, K., Klein, M., 2017. Modeling and simulation of water flow on containment walls with inhomogeneous contact angle distribution. Atw. Internationale Zeitschrift fuer Kernenergie 62 (7), 477–481.

Amend, K., Klein, M., 2018. Development and validation of a CFD wash-off model for fission products on containment walls. Atw. Internationale Zeitschrift fuer Kernenergie 63 (8–9), 469–473.

Ariathurai, R., 1977. Mathematical model of estuarial sediment transportation PhD thesis. University of California.

Bönigke, G. et al., 1998. Untersuchung von Maßnahmen des anlageninternen Notfall-schutzes zur Schadensbegrenzung in LWR, GRS-A-2601, April.

Freitag, M., Schmidt, E., Gupta,S., Laufenberg, B. von, Colombet, M., Kühnel, A., 2016, Wash-Down Behavior of Silver Aerosols Test AW-3 (Part 1). 1501455-TR-AW-3 (Part 1), Becker Technologies (Jan. 2016).

Freitag, M., Gupta, S., Beck, S., Sonnenkalb, M., 2018. Experimental and analytical investigations of aerosol processes—wash-out and wash-down. Nucl. Sci. Eng. 193, 198–210. https://doi.org/10.1080/00295639.2018.1479091.

Guo, J., 2002. Hunter rouse and shields diagram. Adv. Hydraul. Water Eng. 2, 1096–1098. https://doi.org/10.1142/9789812776969_0200.

Gupta, S., Langer. G, 2009. Aerosol Wash-down Test (AW), OECD-NEA THAI Project , Report No. 1501326–AW-QLR, Becker Technologies, December 2009.

Gupta, S., Balewski, B., et al, 2012. Wash-down Behaviour of Soluble and Non-soluble Aerosols Test ID: AW-2. Report No. 1501361–TR-AW-2, Becker Technologies, November 2012.

Gupta, S., Funke, F., Langrock, G., Weber, G., von Laufenberg, B., Schmidt, E., Freitag, M., Poss, G., 2015. THAI experiments on volatility, distribution and transport behaviour of iodine and fission products in the containment. In: Proceedings of the International OECD-NEA/NUGENIA-SARNET Workshop on the Progress in Iodine Behaviour for NPP Accident Analysis and Management, pp. 1–4.

Hillebrand, G., 2008. Transportverhalten kohäsiver Sedimente in turbulenten Strömungen: Untersuchungen im offenen Kreisgerinne. PhD Thesis, Universität Fridericiana zu Karlsruhe (TH).

Kelm, S., Broxtermann, P., Krajewski, S., Allelein, H.-J., Preusser, G., Sangiorgi, M., 2013. Generic Containment a detailed comparison of containment simulations performed on plant scale. In: 15th Int. Top. Meet. Nucl. React. Therm. - Hydraul. NURETH-15.

Kelm, S., Broxtermann, P., Krajewski, S., Allelein, H.-J., Preusser, G., Sangiorgi, M., et al., 2014. Generic Containment a detailed comparison of containment simulations performed on plant scale. Ann. Nucl. Energy 74, 165–172.

Klein-Heßling, W., Arndt, S., Weber, G., Nowack, H., Spengler, C., Schwarz, S., Pelzer, M., Eckel, J., 2015. COCOSYS v2.4 User's Manual. GRS.

Povilaitis, M., Kelm, S., Urbonavičius, E., 2017. The Generic Containment SB-LOCA accident simulation: comparison of the parameter uncertainties and user-effect. Ann. Nucl. Energy 106, 1–10.

Sangiorgi, M., Grah, A. and Ammirabile, L., 2015. Circuit and Containment Aspects of PHÉBUS Experiment FPT-2. Final Interpretation Report, 2015.

Shields, A., 1936. Anwendung der Aehnlichkeitsmechanik und der Turbulenzforschung auf die Geschiebebewegung. PhD Thesis Technical University Berlin.

Wang, F., Cheng, X., 2019. Modeling approach of flowing condensate coverage rate on inclined wall for aerosol wash-down. Nucl. Eng. Des. 355, (2019) 110349.

Wang, F., Cheng, X., 2020. Extension and validation of aerosol wash-down model on inclined wall. Ann. Nucl. Energy 144, 107506.

Weber, G., 2011. Ein neues Abwaschmodell für unlösliche Aerosole (AULA), GRS-TN-WEG-01/2011, Aug.

Weber, G., Funke, F., Gupta, S., 2015. Iodine and Silver Wash-Down Modelling in Cocosys-Aim By Use of Thai Results. OECD NEA/NUGENIA-SARNET Workshop on the Progress in Iodine Behaviour for NPP Accident Analysis and Management, Marseille, France.